ACS OMEGA

http://pubs.acs.org/journal/acsodf

Article

Synthesis of Covalently Modified Energetic Graphene Oxide/CuO Composites with Enhanced Catalytic Performance for Thermal Decomposition of Ammonium Perchlorate

Dayong Li,* Yuling Shao, Haibo Ke, Shengquan Chang, Yong Kou, Lei Xiao, and Gazi Hao*

Cite This: *ACS Omega* 2023, 8, 22876−22886

Read Online

ACCESS | Metrics & More | Article Recommendations

ABSTRACT: In this study, a new covalently modified energetic graphene oxide (CMGO) was synthesized by introducing the energetic component 4-amino-1,2,4-triazole on GO sheets through valence bond bonding. The morphology and structure of CMGO were studied by scanning electron microscopy, energy-dispersive spectroscopy, Fourier transform infrared spectroscopy, Raman spectroscopy, X-ray diffractometry, and X-ray photoelectron spectroscopy, and the results showed that CMGO was successfully synthesized. Then, CMGO/CuO was prepared by loading nano-CuO onto CMGO sheets using an ultrasonic dispersion method. Furthermore, the catalytic effect of CMGO/CuO on the thermal decomposition of ammonium perchlorate (AP) was investigated using differential scanning calorimetric technique and thermogravimetric analysis. The results revealed that the high decomposition temperature T_H and Gibbs free energy $\Delta G^{\ddagger}$ of the CMGO/CuO/AP composite decreased by 93.9 °C and 15.3 kJ/mol compared with those of raw AP, respectively. The CMGO/CuO composite exhibited more significant catalytic effect on the thermal decomposition of AP than GO/CuO, and the heat release Q of CMGO/CuO/AP was greatly increased from 132.9 to 1428.5 J/g with 5 wt % CMGO/CuO. The above results demonstrated that CMGO/CuO is an excellent composite energetic combustion catalyst, which is expected to be widely used in composite propellants.

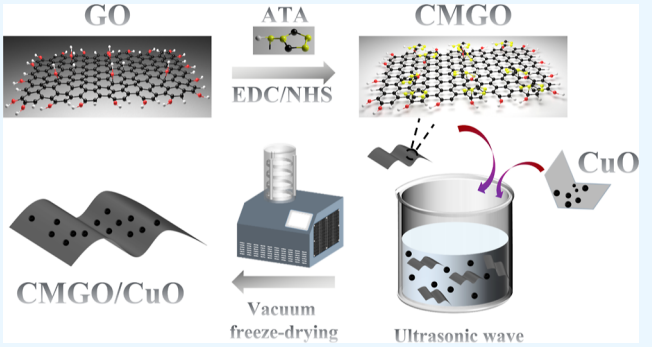

1. INTRODUCTION

Ammonium perchlorate (AP) is an excellent oxidizer with a high effective oxygen content, good thermal stability, and chemical stability, and it has been widely used in composite solid propellants, accounting for about 60−90% of the system.[1−4] Relevant studies have shown that the energy output of propellant systems is largely affected by the combustion performance of AP, so it is necessary to improve the combustion performance of AP as much as possible to effectively increase the energy output of the propellant.[5−7]

In recent decades, transition metals and transition-metal oxides have been widely used to accelerate the thermal decomposition of AP due to their good catalytic performance.[8−10] Among the transition-metal oxides, CuO has attracted considerable attention due to its good catalytic activity, chemical stability, and environmental friendliness.[11−14] The morphology and structure of CuO are also the key factors affecting its catalytic performance. For example, CuO nanoparticles can improve the catalytic performance of AP due to its larger specific surface area and more catalytic active sites.[15,16] However, as said "every coin has two sides", nano-CuO also has fatal defects even if it has excellent catalytic properties on AP. Nano-CuO has a serious agglomeration phenomenon due to its high surface energy and small particle size. This problem would significantly reduce the catalytic active sites exposed on the surface of the nano-CuO, resulting in a decrease in the catalytic performance.

Numerous researchers have conducted a large number of experiments to solve the agglomeration of nano-CuO and improve its catalytic activity. For instance, Fertassi[17] successfully prepared G/CuO nanocomposite by loading CuO nanosheets on graphene (G) sheets using a simple hydrothermal method. The results show that the G/CuO nanocomposite reduced the decomposition temperature of AP from 432 to 325 °C, which was 25 °C earlier than that of single-component CuO. The apparent activation energy was also significantly reduced from 129 to 71.47 kJ/mol, indicating that CuO loaded on graphene sheets had a better catalytic effect. Zhu[18] formed a CuO/GO nanocomposite by loading

Received: March 20, 2023
Accepted: May 30, 2023
Published: June 9, 2023

nano-CuO particles on GO sheets with an in situ deposition method. It was found that the high decomposition temperature (T_H) and heat release (Q) of the nanocomposite was 315 °C and 1347 J/g in the presence of 2 wt % CuO/GO (the mass ratio of CuO to GO was 2:1), demonstrating the excellent catalytic performance of CuO/GO nanocomposite on AP. This approach takes advantage of the large specific surface area of graphene oxide to improve the dispersion of metal oxide nanoparticles, which effectively solves the agglomeration problem and promotes the extensive use of metal oxide combustion catalysts in propellants.

Nowadays, improving the energy output of solid propellants is one of the tasks that need to seek breakthroughs in the research and application, and it is an effective way to introduce combustion catalysts with energetic components into the propellant.[19−23] This is due to the ability of energetic combustion catalysts to modulate the combustion performance of the propellant and to increase its energy output. Moreover, some studies have shown that adding about 3 wt % energetic combustion catalysts into the propellant can improve the specific impulse of the system by 1−3 s, which greatly compensates for the energy loss caused by the introduction of inert combustion catalysts.[21,24] The GO sheets contained many oxygen-containing functional groups (such as hydroxyl and carboxyl groups), which provides the possibility to carry out many functional modifications such as esterification and amidation.[25−28] Hostert[29] obtained the imidazole (IMZ)-functionalized GO (GOIMZ) by modifying 1-(3-aminopropyl) imidazole (API) on the GO surface via an amide bond, using 1-ethyl-3-(3-dimethylaminopropyl) carbodiimide (EDC) and *N*-hydroxysuccinimide (NHS) for activating the carboxylate sites of GO. Furthermore, Sa'at[30] successfully prepared functionalized graphene oxide (f-GO) by covalently modifying phenylisocyanate on the surface of GO, and then obtained a catocene/f-GO composite catalyst through physical interaction between catocene and GO. By means of covalent modification, energetic components are modified on the surface of GO, so as to promote the perfect combination of excellent physical and chemical properties between GO and energetic materials.[31,32]

In this study, 4-amino-1,2,4-triazole (ATA) with the amino group ($-NH_2$) was chosen as the energetic component to obtain covalently modified high-energy graphene (CMGO) by functionalizing the oxygen-containing groups on the surface of GO through nucleophilic substitution.[33−35] Further, nano-CuO particles were dispersed on the surface of CMGO by an ultrasonic dispersion method, and the covalently modified energetic graphene/nano-CuO (CMGO/CuO) was obtained. The prepared CMGO/CuO composite has two unique advantages: CMGO has the energy to increase the energy output of the system, and the layered structure and large specific surface area of CMGO can also greatly reduce the agglomeration of nano-CuO particles, thus effectively exerting the catalytic activity of nano-CuO. In addition, the combination of CMGO and nano-CuO effectively solves the defect of limited catalytic ability of a single component and gives full play to the synergistic catalytic ability of two components, which is expected to be widely used in the propellants.

2. EXPERIMENTAL SECTION

2.1. Materials. AP was purchased from Dalian Perchloric Acid Ammonium Factory. CuO was supplied by Sinopharm Chemical Reagent Co. Ltd. GO was purchased from Suzhou Tanfeng Graphene Technology Co., Ltd. 1-Ethyl-3-(3-dimethylaminopropyl) carbodiimide (EDC), *N*-hydroxysuccinimide (NHS), 4-amino-1,2,4-triazol, and triethylamine were purchased from Shanghai Macklin Biochemical Co., Ltd. Methanol and ethyl acetate were purchased from Nanjing Chemical Reagent Co., Ltd. All reagents are of analytical grade and were used directly without further purification.

2.2. Synthesis of CMGO. First, the dispersed graphene oxide solution (0.5 mg/mL) was obtained by adding graphene oxide into deionized water and ultrasonically dispersing it at 20 °C for 30 min. Then, the crosslinking agent EDC/NHS was added to the GO solution at a dosage of 0.3 mmol/1 mg GO (the molar ratio of EDC to NHS was 1.5:1) in the stirred state, and the reaction lasted for 30 min to obtain the mixed solution. Further, the PH of the solution was adjusted to 7.0 by adding some triethylamine to the mixed solution. Then, the pre-prepared deionized water dispersion of ATA (ATA dosage: 5.04/1 mg GO) was slowly added to the mixed system after the reaction continued for 2 h. Next, the solution was stirred at 50 °C for 12 h, and the product was separated by centrifugation after complete cooling. Finally, the product was washed repeatedly with deionized water and methanol 5 times and freeze-dried in vacuum for 24 h to obtain CMGO. The schematic diagram of the preparation of CMGO can be observed shown in Figure 1. The type and proportion of the crosslinker and the pH of the solution are all important factors in the synthesis of CMGO; it is essential to select raw materials and conduct experiments based on the nature of the crosslinker itself and the interaction between the different substances.

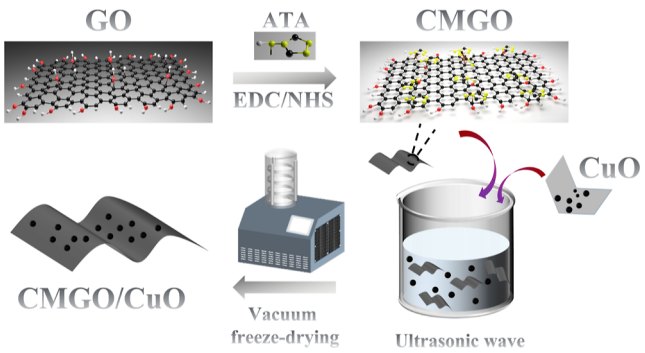

Figure 1. Schematic diagram of the preparation of CMGO.

2.3. Synthesis of CMGO/CuO. CMGO/CuO was prepared by the ultrasonic dispersion method. First, 0.05 g of CMGO was weighed into a beaker with 30 mL of deionized water, and a homogeneous CMGO suspension could be obtained by ultrasonic dispersion for 30 min. Next, 0.05 g of nano-CuO was added in 20 mL of deionized water and ultrasonicated for 30 min to obtain the suspension of nano-CuO. It is worth noting that the mass ratio of CMGO and nano-CuO is 1:1. Then, the suspension of nano-CuO was slowly poured into the suspension of CMGO under the condition of stirring, and the mixed suspension was placed in the magnetic stirrer for mixing and stirring for 2 h. Finally, the CMGO/CuO could be obtained by vacuum freeze-drying for 12 h. Furthermore, GO/CuO was obtained with the same mass ratio and the above preparation method. The preparation process of CMGO and CMGO/CuO is shown in Figure 1.

https://doi.org/10.1021/acsomega.3c01865
ACS Omega 2023, 8, 22876−22886

2.4. Synthesis of Different Composites. The CMGO/CuO/AP composite was synthesized by the mechanical grinding method. AP was dried in an oven for 24 h before the experiments. First, CMGO/CuO and pure AP were added to a mortar with the mass ratio of 5:95, then the samples were mixed by slow grinding after adding 1 mL of ethyl acetate. It is worth noting that the grinding strength should be controlled to avoid changing the size of the particles. Finally, the CMGO/CuO/AP composite containing 5 wt % CMGO/CuO was obtained by drying in an oven at 60 °C for 20 min. Furthermore, GO/CuO/AP, CMGO/AP, CuO/AP, and GO/AP can be prepared with the same mass ratio and the same method.

2.5. Measurements. Scanning electron microscopy (SEM) tests were performed using a high-resolution thermal field scanning electron microscope (Quanta 400 F). Fourier transform infrared (FT-IR) of the samples was carried out (Nicolet iS10) in the range of 4000−500 cm^{-1}. Raman spectrometry was performed with a LabRam HR Evolution instrument equipped with a 532 nm laser wavelength. The crystal forms of the samples were determined using an Advanced D8 X-ray diffractometer. In addition, X-ray photoelectron spectroscopy (XPS) measurements were performed using an ESCALAB 250Xi spectrometer equipped with a pass energy of 30 eV, a power of 100 W (10 kV and 10 mA) and a monochromatized Al Kα X-ray source. The thermal analysis experiment was performed using a METTLER TOLEDO TGA/DSC3+ system; the N_2 flow rate was 50 mL/min, the selected heating rate was 5, 10, 15, and 20 °C/min, and the system was heated from 50 to 500 °C. The kinetic parameters for the exothermic decomposition of pure AP and AP composites were obtained using the Kissinger method.[36]

3. RESULTS AND DISCUSSION

3.1. Micromorphology of Composites. The micromorphology of different composites was investigated by SEM, and the results are shown in Figure 2. Figure 2a shows that GO presents curled clusters and folded sheets, which may be caused by the uneven oxidation degree on the surface of GO during the preparation process, and the form of GO resembles the shape of silk during dancing. As shown in Figure 2b, the surface folds of CMGO increased significantly, which was caused by the destruction of the integrity of the graphene lattice during the covalent modification of graphene oxide, and it led to the uneven distribution of surface tension of graphene oxide. Figure 2c shows that the CuO nanoparticles are spherical with uniform particle size distribution, but there is an obvious agglomeration phenomenon, which could significantly reduce its catalytic performance. Figure 2d,e shows the microscopic morphology of GO/CuO and CMGO/CuO composites, and nano-CuO is well loaded on GO and CMGO. The good dispersion of nano-CuO on the surface of CMGO facilitates the synergistic catalysis between CMGO and CuO.[6,8]

Elemental analysis was used to characterize the combination effect of the two composites, as the SEM images of GO/CuO and CMGO/CuO show similar microscopic morphologies, and the results are shown in Figure 3. It clearly shows that GO/CuO contains the three elements C, O, and Cu. The three elements can be observed at different positions in the image, inferring that nano-CuO was uniformly dispersed on the surface of GO. CMGO/CuO exhibits a more uniform distribution of elements, and the presence of N element

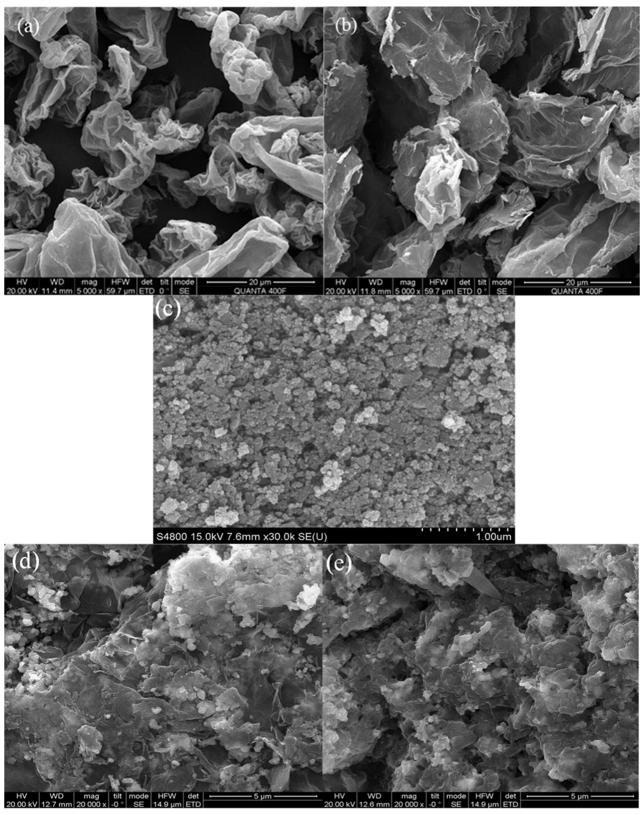

Figure 2. SEM images of different samples: (a) GO; (b) CMGO; (c) CuO; (d) GO/CuO; and (e) CMGO/CuO.

confirms the successful preparation of CMGO. It can also be found that the distribution of different elements in CMGO/CuO is denser than that of GO/CuO, especially the Cu element. The above conclusions demonstrate that CuO nanoparticles can be better combined with CMGO, resulting in a more uniform dispersion of nano-CuO on CMGO, which is related to the ATA on the surface of GO.[8,23]

3.2. Structures of Different Samples. The structures of GO, CMGO, CuO, GO/CuO, and CMGO/CuO were analyzed using FT-IR and Raman to verify the successful modification of ATA on GO sheets using covalent bonds, and the results are shown in Figure 4. As can be seen in the spectrogram, GO shows characteristic peaks at 1052, 1224, 1735, 3386 cm^{-1}, etc. The characteristic absorption peak of GO at 1052 cm^{-1} is associated with the anti-symmetric stretching vibration of C−O−C, and the characteristic absorption peaks at 1224 and 1735 cm^{-1} correspond to C−OH and C═O, respectively. The characteristic peak at 3386 cm^{-1} is attributed to the stretching vibration of the O−H bond in GO. CMGO shows distinctive characteristic peaks at 954, 1048, 1381, 1563, 1648 cm^{-1}, etc. Among them, the characteristic absorption peak at 1648 cm^{-1} corresponds to the bending vibration of N−H. The new vibrational absorption peak of CMGO near 1381 cm^{-1} is associated with the bending vibration of C−N. The C−N may be derived from the amide bond (−CO−NH−) formed by the covalent modification of GO and ATA, and it may also be the C−N bond in the energetic component of ATA. The new absorption vibrational peaks at 1563 and 954 cm^{-1} correspond to the skeletal vibration of the triazole ring in ATA, which proves the presence of ATA in energetic graphene. In addition, the absorption peak of GO at 1052 cm^{-1} is the anti-symmetric

https://doi.org/10.1021/acsomega.3c01865
ACS Omega 2023, 8, 22876−22886

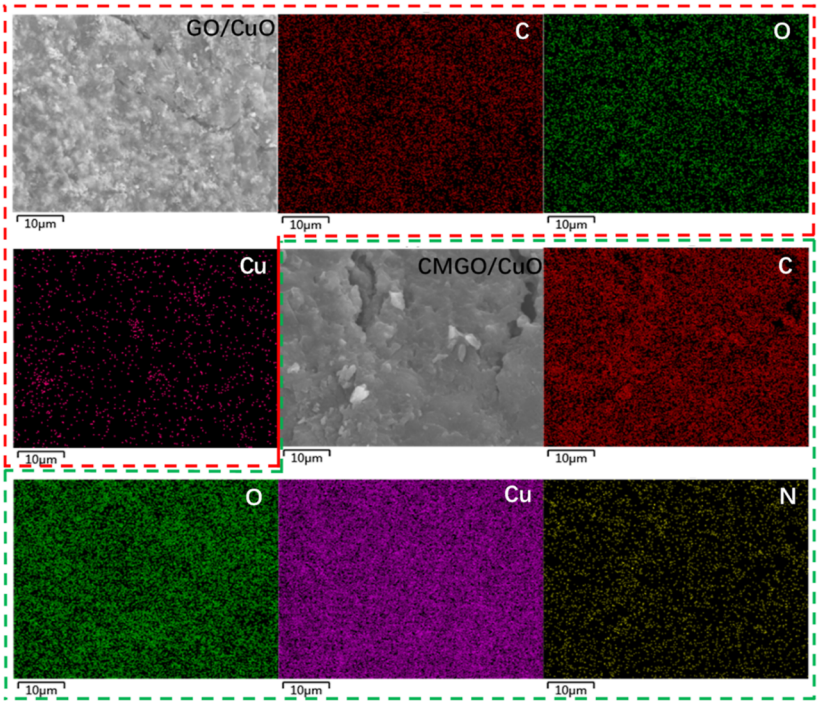

Figure 3. Mapping patterns of GO/CuO and CMGO/CuO.

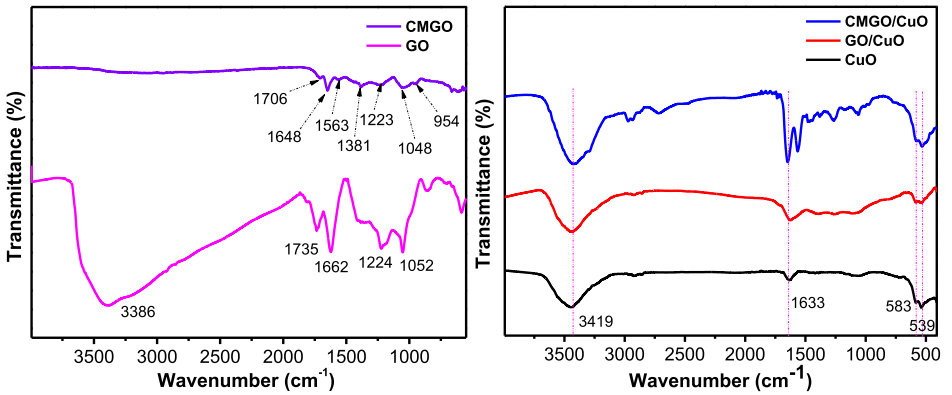

Figure 4. FT-IR spectra of GO and CMGO.

stretching vibration absorption peak of C−O−C, corresponding to the absorption peak of energetic graphene at 1048 cm^{-1}. The epoxy group (C−O−C) in GO may also undergo a ring-opening reaction with the amino group ($-NH_2$) in ATA, resulting in a significant reduction of the absorption peak intensity observed for CMGO. The nano-CuO exhibits strong characteristic peaks at around 3419, 1633, 583, and 539 cm^{-1}. The peaks located at 3419 and 1633 cm^{-1} are attributed to stretching and bending vibrational peaks of the O−H bond, which may be caused by a small amount of water molecules adsorbed on the surface of the nano-CuO. The diffraction peaks at 583 and 539 cm^{-1} are assigned to the stretching vibration of the Cu−O bond. In the GO/CuO composite, the characteristic peaks of both GO and CuO were observed simultaneously without any additional diffraction peaks, indicating physical mixing between GO and CuO. The diffraction peaks of the CMGO/CuO composite are ascribed to the diffraction peaks of CMGO at 954, 1048, 1223, 1381, 1563, 1648, and 1706 cm^{-1}, as well as the characteristic peaks of CuO at 3419, 1633, 583, and 539 cm^{-1}, indicating the successful preparation of the CMGO/CuO physical mixture.[17,18,37,38]

Raman spectra of GO and CMGO are shown in Figure 5. As can be seen in Figure 5, the D-peak of the GO sheet at 1346 cm^{-1} reflects its characteristic of disorder. The characteristic

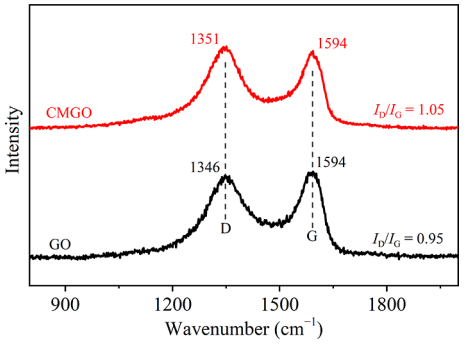

Figure 5. Raman spectra of GO and CMGO.

https://doi.org/10.1021/acsomega.3c01865
ACS Omega 2023, 8, 22876−22886

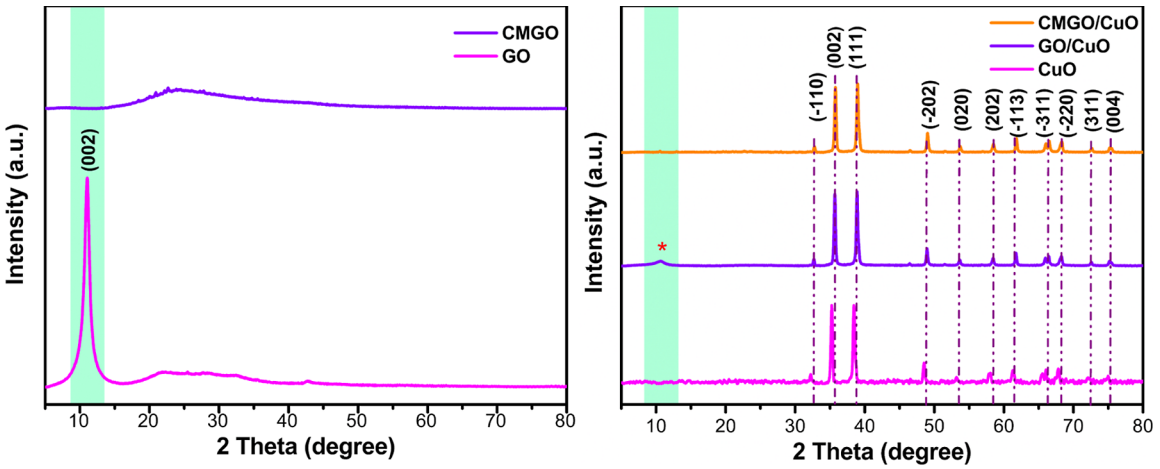

Figure 6. XRD patterns of different samples.

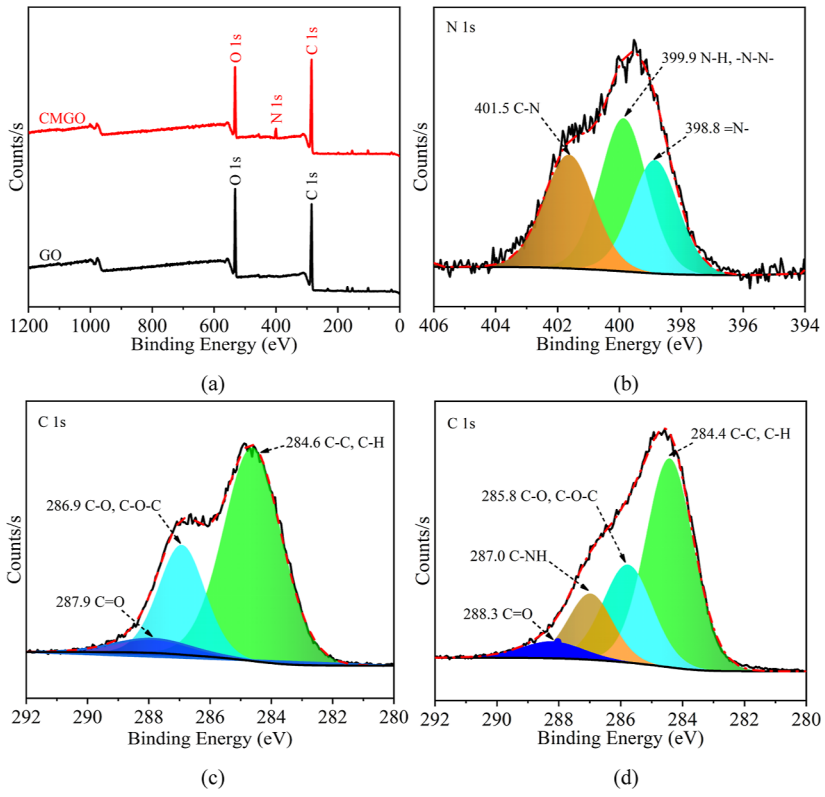

Figure 7. XPS (a) survey spectra of GO and CMGO; (b) peak-fitting spectra of N 1s of CMGO; (c) peak-fitting spectra of C 1s of GO; and (d) peak-fitting spectra of C 1s of CMGO.

peak at 1594 cm^{-1} corresponds to the G-peak of sp^2-hybridized carbon atoms on GO sheets, which reflects the symmetry and crystal integrity of GO. The intensity ratio (I_D/I_G) of the D and G peaks is usually used to probe the degree of defects in GO sheets and the degree of covalent modification of CMGO. The large I_D/I_G ratios imply more covalent bonding of functional groups on the surface and edges of GO and CMGO. It can also be found that the ratio of I_D/I_G in CMGO increases from 0.95 to 1.05, which is due to the disruption of the covalently modified lattice of GO and further increase of defects in the GO sheet. The above phenomena are consistent with the conclusions drawn from SEM, which further confirms the successful preparation of CMGO.[17,18]

Figure 6 shows the X-ray diffraction (XRD) patterns of GO, CMGO, CuO, GO/CuO, and CMGO/CuO. As shown in Figure 6, the most intense peak at around 2θ = 11.04° corresponds to the (002) reflection of GO. It can also be observed that the diffraction peak of GO at (002) disappears due to the introduction of the amino group, confirming the formation of CMGO. A sharper diffraction peak than GO appears in CMGO near 24°, while the tiny diffraction peak at 42.9° disappears, both of which were associated with the successful addition of amino group. The nano-CuO shows strong diffraction peaks at 2θ = 32.2, 35.3, 38.4, 48.5, 53.2, 58.1, 61.3, 66.1, 67.8, 72.2, and 75.0°, corresponding to the crystalline planes of (−1 1 0), (0 0 2), (1 1 1), (−2 0 2), (0 2 0), (2 0 2), (−1 1 3), (−3 1 1), (−2 2 0), (3 1 1), and (0 0 4).

https://doi.org/10.1021/acsomega.3c01865
ACS Omega 2023, 8, 22876−22886

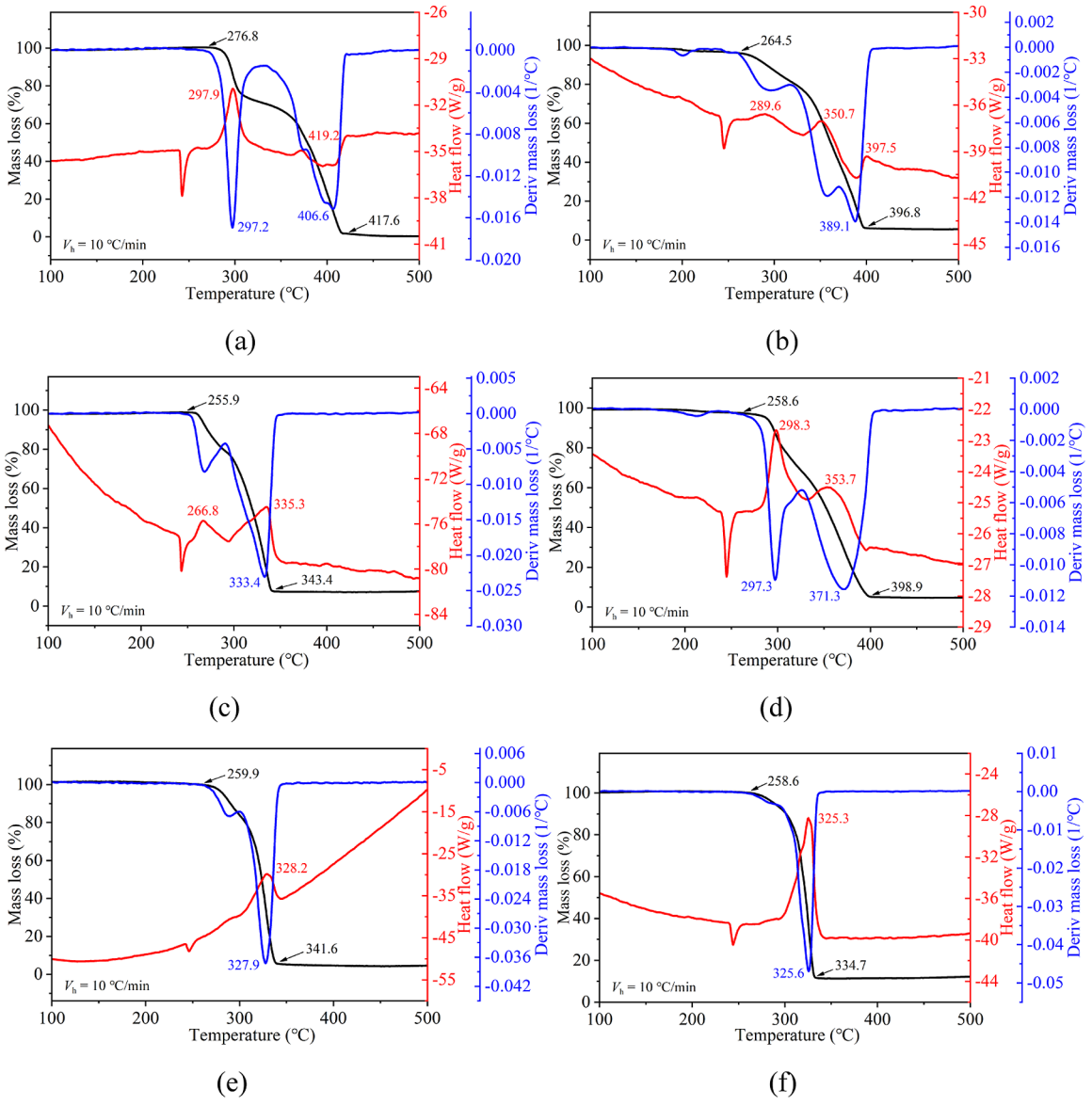

Figure 8. TG−DSC−DTG curves of AP and AP composite samples. (a) AP, (b) GO/AP, (c) CuO/AP, (d) CMGO/AP, (e) GO/CuO/AP, and (f) CMGO/CuO/AP.

The presented diffraction peaks of nano-CuO are consistent with the standard PDF card (PDF: 45-0937), inferring that the crystalline form of the nano-CuO is monoclinic. In the GO/CuO composite, the diffraction peaks of nano-CuO appear with those of GO, confirming that the two samples are physically mixed without chemical interaction, while the lower content of GO leads to a reduction in the intensity of the diffraction peak at (0 0 2). Moreover, it also shows the diffraction peaks of nano-CuO in the CMGO/CuO composite, without additional diffraction peaks being generated and disappeared. The above findings confirm the successful synthesis of CMGO and the physical mixing of GO/CuO and CMGO/CuO.[21,22,37,38]

XPS was employed to verify the chemical-binding relationship between GO and the energetic ligand (ATA), and the results are shown in Figure 7. Figure 7a shows that only two elements (O and C) are detected in GO, while three elements (O, C, and N) appeared in the spectrum of CMGO, and the presence of N at 399.1 eV confirms the successful preparation of CMGO. Figure 7b illustrates the high-resolution spectrum of N 1s region in CMGO. The results demonstrate that the N element in CMGO has three chemical states: 401.5 eV (C−N), 399.9 eV (N−H, −N−N−), and 398.8 eV (=N−), in which N−H, −N−N− and =N− are unique valent-bond fitting peaks of ATA, illustrating the covalent binding of ATA to GO. In addition, Figure 7c displays the high-resolution spectrum of C1 s in GO. It can be found that the C element in GO has three chemical states, which are at 284.6, 286.9, and 287.9 eV, and they are attributed to the sp^2 hybrid lattice carbon (C−C), carbon in epoxy group (C−O−C), and carbon atom on carbonyl group (C=O), respectively. Compared with the C 1s spectra in GO, the content of carbon atoms in CMGO decreased significantly, and a new peak of C−NH at 287.0 eV was generated in Figure 7d. The above findings further demonstrate the successful preparation of CMGO by combining the amino groups in ATA with GO flakes.[8,16,17]

3.3. Catalytic Performance of Different Composites.

TG−DSC−DTG were performed on raw AP and different composites with the heating rate of 10 °C/min to explore the catalytic performance of different samples, and the results are

https://doi.org/10.1021/acsomega.3c01865
ACS Omega 2023, 8, 22876−22886

Table 1. Basic Data of Thermal Decomposition Performance of AP and AP Composite Samples[a]

sample	T_e/°C	T_c/°C	T_m/°C	T_L/°C	T_H/°C	Q/(J/g)
AP	276.8	417.6	406.6	297.9	419.2	132.9
GO/AP	264.5	396.8	389.1	289.6	397.5	352.1
CuO/AP	255.9	343.4	333.4	266.8	335.3	1101.8
CMGO/AP	258.6	398.9	371.3	298.3	353.7	834.2
GO/CuO/AP	259.9	341.6	327.9		328.2	1180.8
CMGO/CuO/AP	258.6	334.7	325.6		325.3	1428.5

[a]T_e is the initial decomposition temperature; T_c is the terminal decomposition temperature; T_m is the temperature at maximum weight loss; T_L is the low decomposition temperature; T_H is the high decomposition temperature; Q is the heat release.

Table 2. Effect of Different Catalysts on the Thermal Decomposition Performance of AP[a]

			LTD			HTD			
samples	M %	β/°C·min^{-1}	raw AP	composites	decrease of LTD temperature	raw AP	composites	decrease of HTD temperature	refs
AP/GO	20	10 °C·min^{-1}	301.78	261.62	40.16	358.63	350.71	7.92	39
AP/GO + Co + AMTZ	5	10 °C·min^{-1}	312.1			410.7	314.32	96.38	40
AP/CuO	4	20 °C·min^{-1}				441.3	346.6	94.7	41
AP/CuO (flake)	2	20 °C·min^{-1}				424.4	328.3	96.1	42
AP/CuO (linear)	2	20 °C·min^{-1}				424.4	327.9	96.5	42
AP/CuO (rod)	2	20 °C·min^{-1}				424.4	321.7	102.7	42
AP/CuO (spherical)	2	20 °C·min^{-1}				424.4	320.3	104.1	42
AP/GO/Fe_2O_3 (1:10)	3	10 °C·min^{-1}				455	378	77	43
AP/GO/Fe_2O_3 (3:20)	3	10 °C·min^{-1}				455	384	71	43
AP/GO/Fe_2O_3 (3:10)	3	10 °C·min^{-1}				455	387	68	43
AP/GO/Fe_2O_3 (1:1)	3	10 °C·min^{-1}				455	408	47	43
AP/GO/Fe_2O_3 (3:1)	3	10 °C·min^{-1}				455	425	30	43
CMGO/AP	5	10 °C·min^{-1}	297.9	298.3	+0.4	419.2	353.7	65.5	this work
CMGO/CuO/AP	5	10 °C·min^{-1}	297.9			419.2	325.3	93.9	this work

[a]Low-temperature decomposition (LTD); high-temperature decomposition (HTD).

shown in Figure 8. The basic data on the thermal decomposition properties of the different samples are shown in Table 1.

As can be seen in Figure 8 and Table 1, there are two decomposition stages in the thermal decomposition of AP; the peak at 297.9 °C is the low-temperature decomposition peak of AP, and the peak at 419.2 °C is the high-temperature decomposition peak of AP. GO, CMGO, and CuO nanoparticles all exhibit a significant catalytic effect on AP, resulting in a significant decrease in the thermal decomposition temperature of AP and a considerable increase in its heat release, especially the nano-CuO. The high-temperature decomposition peak of GO/CuO/AP is significantly advanced due to the presence of 5 wt % GO/CuO. When using 5% CMGO/CuO rather than GO/CuO as the catalyst for AP, the high-temperature decomposition peak of AP was found to overlap with its low-temperature decomposition peak. The T_H of GO/CuO/AP advances from 419.2 to 328.2 °C, which is 69.3 °C earlier than that of the GO/AP composite, and it is also 7.1 °C earlier than that of the CuO/AP composite. The above conclusions fully demonstrate the excellent synergistic catalytic effect of GO and CuO. Furthermore, the T_m value of GO/CuO/AP is also significantly advanced, which also indicates the good catalytic effect of the GO/CuO composite. The introduction of GO improves the dispersion of nano-CuO particles and inhibits the agglomeration of CuO nanoparticles, which improves the overall catalytic activity. The advance values of T_e (259.9 °C) and T_c (341.6 °C) also indicate that the GO/CuO composite is more conducive to accelerate the thermal decomposition of AP. As shown in Table 1, the heat release of the GO/CuO/AP composite (1180.8 J/g) is significantly higher than that of AP (132.9 J/g) and other composites. In addition, the CMGO/CuO/AP composite also shows a huge advantage in heat release (1428.5 J/g), and it is about 1.2 times higher than that of the GO/CuO/AP composite. These results indicate that the CMGO/CuO composite not only inherits the excellent catalytic performance of the GO/CuO composite but also greatly improves the overall energy output of the AP system. Furthermore, the CMGO/GO composite has better catalytic effect and higher heat release for AP, indicating that it is a good composite energetic combustion catalyst.[9−11]

https://doi.org/10.1021/acsomega.3c01865
ACS Omega 2023, 8, 22876−22886

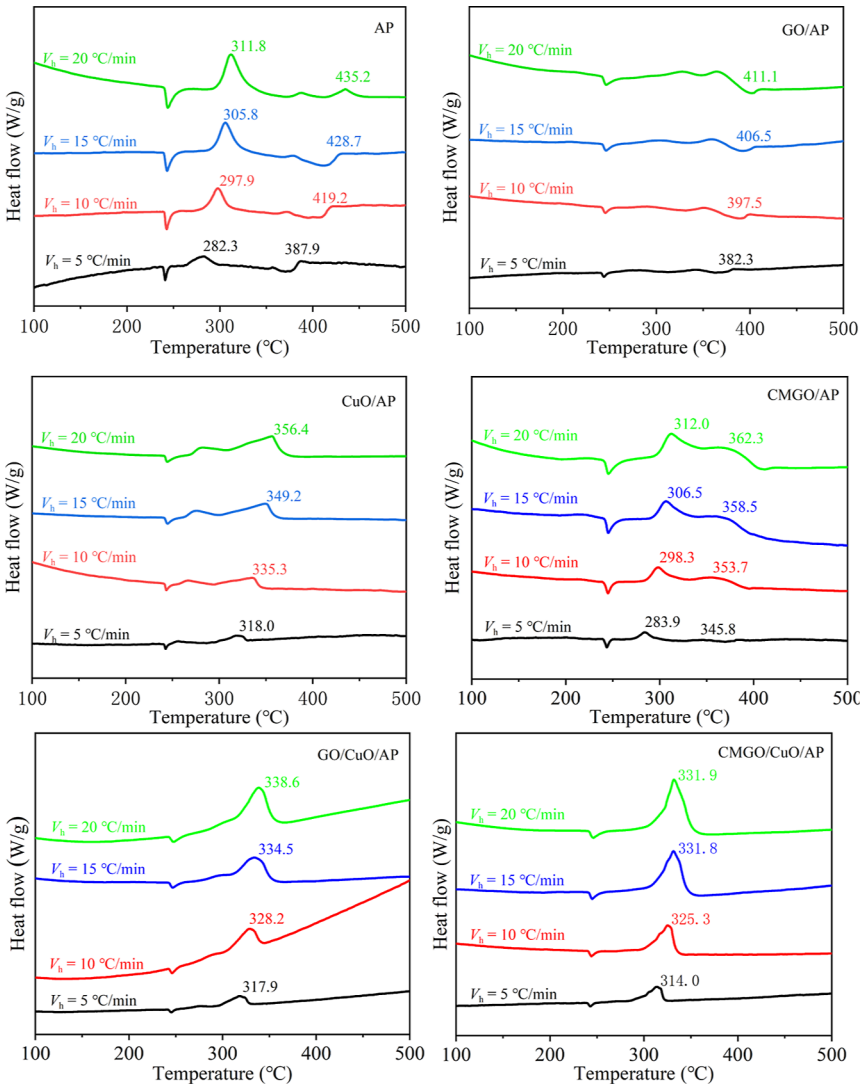

Figure 9. DSC curves of AP and AP composite samples at different heating rates.

In addition, the catalytic effect of the CMGO and CMGO/CuO prepared in this study was compared with the catalytic effect of different catalysts in the literature, and the results are shown in Table 2. It clearly shows that various catalysts provided good catalysis for the thermal decomposition of AP, especially the high-temperature decomposition (HTD) peak of AP. It can also be found that CMGO shows better catalytic effect on AP than GO, and the dispersion of CuO on the surface of CMGO also exerts an excellent catalytic effect on AP, even with a low content of CuO.

To further study the pyrolysis of AP and different composites, DSC tests were carried out on different samples at different heating rates, and the results are shown in Figure 9. As can be seen in Figure 9, the thermal decomposition temperature of different samples shows a significant hysteresis effect with the increase of the heating rate, which was caused by the uneven heating of the samples when the heating rate was increased. GO, CMGO, and CuO all have catalytic effects on AP and advance its exothermic peak. GO/CuO and CMGO/CuO have more obvious synergistic catalytic effect on AP with only one significant exothermic peak. Especially, the CMGO/CuO/AP composite has the largest exothermic peak, confirming the obvious catalytic performance of CMGO/CuO on AP.[7]

According to the T_H at different heating rates in Figure 9, a linear fit was performed with $1000/T_p$ and $\ln(\beta/T_2\ P)$ as the horizontal and vertical coordinates, respectively. The $\ln(\beta/T_2\ P)-1000/T_p$ diagram of AP and different composites were obtained, as shown in Figure 10.

The Kissinger method was employed to calculate the thermal decomposition kinetic parameters of AP and different composites, and the equation is shown in eq 1

$$\ln\left(\frac{\beta}{T_p^2}\right) = -\frac{E_a}{RT_p} + \ln\left(\frac{AR}{E_a}\right) \tag{1}$$

where β is the heating rate (K/min), E_a denotes the activation energy (kJ/mol), A is the pre-exponential factor (min^{-1}), and R represents the molar gas constant (8.314 $J{\cdot}mol^{-1}{\cdot}K^{-1}$).

Further, E_a and A of AP and different composites could be obtained according to the linear fitting equations in Figure 10, and the results are summarized in Table 3.

$$T_{p0} = T_{pi} - a\beta_i - b\beta_i^2 - c\beta_i^3 \tag{2}$$

https://doi.org/10.1021/acsomega.3c01865
ACS Omega 2023, 8, 22876−22886

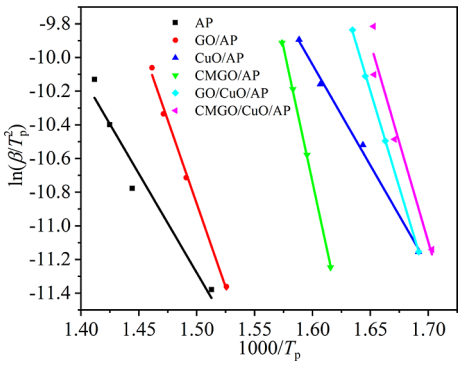

Figure 10. $\ln(\beta/T_2\ P) - 1000/T_p$ diagram of AP and different composite samples.

$$\Delta S^{\ddagger} = R\left[\ln A - \ln \frac{k_B T_{p0}}{h}\right] \quad (3)$$

$$\Delta H^{\ddagger} = E_a - RT_{p0} \quad (4)$$

$$\Delta G^{\ddagger} = \Delta H^{\ddagger} - T_{p0}\Delta S^{\ddagger} \quad (5)$$

where T_{pi} is the decomposition temperature at the heating rate of β_i, T_{p0} (K) is the decomposition peak temperature at which β tends to 0, k_B represents the Boltzmann constant (1.381×10^{-23} J/K), and h denotes the Planck constant (6.626×10^{-34} J·s); $\Delta S^{\ddagger}$, $\Delta H^{\ddagger}$, and $\Delta G^{\ddagger}$ are the activation entropy, enthalpy and Gibbs free energy, respectively.

The thermal decomposition of raw AP and different composites can be described by $\Delta S^{\ddagger}$, $\Delta H^{\ddagger}$, and $\Delta G^{\ddagger}$, and the peak temperature (T_{p0}) can be calculated from eq 2. Then, eqs 3−5 could be used to calculate the relevant parameters, and the results are shown in Table 3.

As can be seen in Table 3, the $\Delta G^{\ddagger}$ values of GO/CuO/AP and CMGO/CuO/AP are significantly lower than those of AP, GO/AP, CuO/AP, and CMGO/AP. Among them, CMGO/CuO/AP shows the lowest $\Delta G^{\ddagger}$ value (168.2 kJ/mol), indicating that the CMGO/CuO/AP composite is more susceptible to thermal decomposition than the other samples, suggesting a more significant catalytic effect of CMGO/CuO on AP. The $\Delta S^{\ddagger}$ values of GO/CuO/AP and CMGO/CuO/AP are 28.2 and 40.8 J·mol^{-1}·K^{-1}, respectively, which are significantly higher than those of AP and other composites, indicating that the GO/CuO/AP and CMGO/CuO/AP systems have a higher disorder of the system when the activation of the molecules occurs. In addition, it can also be found that the T_{p0} values of CuO/AP (300.6 °C), GO/CuO/AP (301.8 °C), and CMGO/CuO/AP (299.2 °C) are significantly advanced, especially the CMGO/CuO/AP composite. The above phenomenon fully demonstrates the more obvious catalytic performance of CMGO/CuO on AP.[23]

4. CONCLUSIONS

In this study, the energetic components (ATA) were successfully modified on GO sheets to obtain CMGO through covalent modification, and then nano-CuO was loaded on the surface of GO and CMGO through the ultrasonic dispersion method to obtain the new composite energetic combustion catalysts of GO/CuO and CMGO/CuO. The results of SEM, EDS, IR, Raman, and XRD confirmed the successful preparation of the composite catalyst. The CuO nanoparticles were uniformly dispersed on the surface of CMGO, as well as GO. Furthermore, TG and DSC were used to investigate the catalytic performance of GO, CuO, CMGO, GO/CuO, and CMGO/CuO on AP. The results showed that CMGO/CuO has a more significant catalytic effect on the thermal decomposition of AP than GO/CuO due to the fact that CMGO is an energetic combustion catalyst, and the heat release of AP considerably increased with 5 wt % CMGO/CuO from 132.9 to 1428.5 J/g. The excellent catalytic effect of CMGO/CuO was attributed to the synergistic catalytic effect of CMGO and CuO. Furthermore, the nano-CuO loading on CMGO greatly improved its dispersion and facilitated its catalytic performance on AP. Overall, these results show that the successful preparation of CMGO/CuO provides a basis for the development of composite energetic combustion catalysts, and the CMGO/CuO composite prepared in this study is expected to be widely used in the field of propellants. For example, the synthesized CMGO, as an energetic material, can be used directly as a combustion catalyst for propellants to improve the thermal decomposition and combustion performance of propellants. In addition, CMGO can be used as a carrier for combustion catalysts to improve the dispersion of the nanocatalysts, thus giving full play to the catalytic effect of nanocatalysts and improving the performance of propellants.

AUTHOR INFORMATION

Corresponding Authors

Dayong Li − *China North Chemical Research Institute Group Co., Ltd., Beijing 100000, China*; Email: 43070531@qq.com

Gazi Hao − *National Special Superfine Powder Engineering Research Center of China, School of Chemistry and Chemical Engineering, Nanjing University of Science and Technology, Nanjing 210094, China*; orcid.org/0000-0002-6508-5274; Email: hgznjust1989@163.com

Authors

Yuling Shao − *China North Chemical Research Institute Group Co., Ltd., Beijing 100000, China*

Haibo Ke − *National Special Superfine Powder Engineering Research Center of China, School of Chemistry and Chemical Engineering, Nanjing University of Science and Technology, Nanjing 210094, China*

Table 3. Kinetics, Thermodynamics, and Thermal Stability Parameters of AP and Different Composites

sample	T_{p0} (°C)	ln A (min^{-1})	E_a (kJ/mol)	$\Delta S^{\ddagger}$ (J·mol^{-1}·K^{-1})	$\Delta H^{\ddagger}$ (kJ/mol)	$\Delta G^{\ddagger}$ (kJ/mol)
AP	316.0	15.8	97.9	−153.6	93.0	183.5
GO/AP	359.1	28.8	164.9	−45.9	159.7	188.7
CuO/AP	300.6	18.5	99.5	−130.7	94.7	169.7
CMGO/AP	332.7	50.7	265.6	137.1	260.6	177.5
GO/CuO/AP	301.8	37.6	190.3	28.2	185.5	169.3
CMGO/CuO/AP	299.2	39.1	196.3	40.8	191.6	168.2

https://doi.org/10.1021/acsomega.3c01865
ACS Omega 2023, 8, 22876−22886

Shengquan Chang − *Liaoning Qingyang Special Chemical Co., Ltd., Liaoyang 111000, China*
Yong Kou − *National Special Superfine Powder Engineering Research Center of China, School of Chemistry and Chemical Engineering, Nanjing University of Science and Technology, Nanjing 210094, China*
Lei Xiao − *National Special Superfine Powder Engineering Research Center of China, School of Chemistry and Chemical Engineering, Nanjing University of Science and Technology, Nanjing 210094, China*

Complete contact information is available at: https://pubs.acs.org/10.1021/acsomega.3c01865

Notes

The authors declare no competing financial interest.

■ ACKNOWLEDGMENTS

This work was financially supported by the National Natural Science Foundation of China (no. 21805139), the Youth Scientific and Technological Innovation Project, and the Young Elite Scientists Sponsorship Program by CAST (program, 2021QNRC001).

■ REFERENCES

(1) Wang, J.; Jin, L.; Qian, X.; Dong, M. Preparation and catalytic activity comparison of porous NiO, Co_3O_4 and $NiCo_2O_4$ superstructures on the thermal decomposition of ammonium perchlorate. *J. Nanosci. Nanotechnol.* **2016**, *16*, 8635−8639.
(2) Nagendra, K.; Vijay, C.; Ingole, M.; Ramakrishna, P. A. Combustion of Ammonium Perchlorate monopropellant: Role of heat loss. *Combust. Flame* **2019**, *209*, 363−375.
(3) Yu, C.; Zhang, W.; Gao, Y.; Chen, Y.; Ma, K.; Ye, J.; Shen, R.; Yang, Y. Shape-controlled syntheses of Co_3O_4 nanowires arrays with excellent catalytic performances upon ammonium perchlorate decomposition. *Mater. Res. Bull.* **2018**, *97*, 483−489.
(4) Zhang, Y.; Meng, C. Facile fabrication of Fe_3O_4 and Co_3O_4 microspheres and their influence on the thermal decomposition of ammonium perchlorate. *J. Alloys Compd.* **2016**, *674*, 259−265.
(5) Chaturvedi, S.; Dave, P. N. A review on the use of nanometals as catalysts for the thermal decomposition of ammonium perchlorate. *J. Saudi Chem. Soc.* **2013**, *17*, 135−149.
(6) Yan, Q.; Zhao, F.; Kuo, K. K.; Zhang, X.; Zeman, S.; DeLuca, L. T. Catalytic effects of nano additives on decomposition and combustion of RDX-HMX-and AP-based energetic compositions. *Prog. Energy Combust. Sci.* **2016**, *57*, 75−136.
(7) Liu, D.; Xuan, C.; Xiao, L.; Hu, Y.; Zhang, G.; Zhao, F.; Gao, H.; Jiang, W.; Hao, G. Dense, Three-Dimensional, Highly Absorbent, Graphene Oxide Aerogel Coating on $ZnCo_2O_4$/ZnO Particles Exerts a Synergistic Catalytic Effect for Ammonium Perchlorate Thermal Decomposition. *Langmuir* **2022**, *38*, 15234−15244.
(8) Kou, Y.; Wang, Y.; Zhang, J.; Guo, K.; Song, X. Iron/aluminum nanocomposites prepared by one-step reduction method and their effects on thermal decomposition of AP and AN. *Def. Technol.* **2023**, *22*, 74−87.
(9) Liang, Y.; Li, G. Catalytic activities of two different morphological Co_3O_4 on the thermal decomposition of ammonium perchlorate. *Mater. Res. Express* **2019**, *6*, 0850e8.
(10) Zhang, M.; Zhao, F.; Li, H.; Yang, Y.; An, T.; Jiang, Y.; Li, N. Morphology-dependent catalytic activity of Fe_2O_3 and its graphene-based nanocomposites on the thermal decomposition of AP. *FirePhysChem* **2021**, *1*, 46−53.
(11) Zhang, C.; Li, G.; Luo, Y. Preparation of Al/CuO/PG nanocomposite and catalytic effect on thermal decomposition of AP. *Integr. Ferroelectr.* **2018**, *191*, 151−157.
(12) Liu, P.; Wang, M.; Wang, L.; Wang, J.; Wang, T. Effect of nano-metal oxide and nano-metal oxide/graphene composites on thermal decomposition of potassium perchlorate. *Chem. Pap.* **2019**, *73*, 1489−1497.
(13) Atamanov, M.; Yelemessova, Z.; Imangazy, A.; Kamunur, K.; Lesbayev, B.; Mansurov, Z.; Yue, T.; Shen, R.; Yan, Q. L. The Catalytic Effect of CuO-Doped Activated Carbon on Thermal Decomposition and Combustion of AN/Mg/NC Composite. *J. Phys. Chem. C* **2019**, *123*, 22941−22948.
(14) Ayoman, E.; Hosseini, S. G. Synthesis of CuO nanopowders by high-energy ball-milling method and investigation of their catalytic activity on thermal decomposition of ammonium perchlorate particles. *J. Therm. Anal. Calorim.* **2016**, *123*, 1213−1224.
(15) Chatragadda, K.; Vargeese, A. A. Synergistically catalysed pyrolysis of hydroxyl terminated polybutadiene binder in composite propellants and burn rate enhancement by free-standing CuO nanoparticles. *Combust. Flame* **2017**, *182*, 28−35.
(16) Hosseini, S. G.; Khodadadipoor, Z.; Mahyari, M. CuO nanoparticles supported on three-dimensional nitrogen-doped graphene as a promising catalyst for thermal decomposition of ammonium perchlorate. *Appl. Organomet. Chem.* **2017**, *32*, No. e3959.
(17) Fertassi, M. A.; Alali, K. T.; Liu, Q.; Li, R.; Liu, P.; Liu, J.; Liu, L.; Wang, J. Catalytic effect of CuO nanoplates, a graphene (G)/CuO nanocomposite and an Al/G/CuO composite on the thermal decomposition of ammonium perchlorate[J]. *RSC Adv.* **2016**, *6* (78), 74155−74161.
(18) Zhu, J.; Zeng, G.; Nie, F.; Xu, X.; Chen, S.; Han, Q.; Wang, X. Decorating graphene oxide with CuO nanoparticles in a water−isopropanol system. *Nanoscale* **2010**, *2*, 988−994.
(19) Shao, C.; Li, J.; Wu, S.; Qi, X.; Song, Z.; Liu, F. Influence of high efficient energetic combustion catalyst on combustion performance of double-based propellant. *Chem. Propellants Polym. Mater.* **2011**, *9*, 67−69.
(20) Hanafi, S.; Trache, D.; Meziani, R.; Boukeciat, H.; Tarchoun, A. F.; Abdelaziz, A.; Mezroua, A. Thermal decomposition and kinetic modeling of HNTO/AN-based composite solid propellant in the presence of GO-based nanocatalyst. *FirePhysChem* **2022**, *2*, 315−322.
(21) Zhao, J.; Liu, Z.; Qin, Y.; Hu, W. Fabrication of Co_3O_4/graphene oxide composites using supercritical fluid and their catalytic application for the decomposition of ammonium perchlorate. *CrystEngComm* **2014**, *16*, 2001.
(22) Yan, Q.; Cohen, A.; Petrutik, N.; Shlomovich, A.; Burstein, L.; Pang, S.; Gozin, M. Highly insensitive and thermostable energetic coordination nanomaterials based on functionalized graphene oxides. *J. Mater. Chem. A* **2016**, *4*, 9941−9948.
(23) Kou, Y.; Luo, P.; Xiao, L.; Xin, Y.; Zhang, G.; Hu, Y.; Yang, J.; Gao, H.; Zhao, F.; Jiang, W.; Hao, G. New insights in nano-copper chromite catalyzing ultrafine AP: Evaluation of dispersity and mixing uniformity. *Def. Technol.* 2023, In Press. DOI: 10.1016/j.dt.2023.04.004.
(24) Fitzgerald, R. P.; Brewster, M. Q. Flame and surface structure of laminate propellants with coarse and fine ammonium perchlorate. *Combust. Flame* **2004**, *136*, 313−326.
(25) Avinash, M. B.; Subrahmanyam, K. S.; Sundarayya, Y.; Govindaraju, T. Covalent modification and exfoliation of graphene oxide using ferrocene. *Nanoscale* **2010**, *2*, 1762−1766.
(26) Li, Y.; Alain-Rizzo, V.; Galmiche, L.; Audebert, P.; Miomandre, F.; Louarn, G.; Bozlar, M.; Pope, M. A.; Dabbs, D. M.; Aksay, I. A. Functionalization of graphene oxide by tetrazine derivatives: a versatile approach toward covalent bridges between graphene sheets. *Chem. Mater.* **2015**, *27*, 4298−4431.
(27) Jing, Q.; Liu, W.; Pan, Y.; Silberschmidt, V. V.; Li, L.; Dong, Z. Chemical functionalization of graphene oxide for improving mechanical and thermal properties of polyurethane composites. *Mater. Des.* **2015**, *85*, 808−814.
(28) Li, X.; Cheng, Y.; Zhang, H.; Wang, S.; Jiang, Z.; Guo, R.; Wu, H. Efficient CO_2 capture by functionalized graphene oxide nanosheets as fillers to fabricate multi-permselective mixed matrix membranes. *ACS Appl. Mater. Interfaces* **2015**, *7*, 5528−5537.
(29) Hostert, L.; Blaskievicz, S. F.; Fonsaca, J. E.; Domingues, S. H.; Zarbin, A. J.; Orth, E. S. Imidazole-derived graphene nanocatalysts for

organophosphate destruction: Powder and thin film heterogeneous reactions. *J. Catal.* **2017**, *356*, 75−84.
(30) Sa'at, M.; Yarmohammadi, M.; Zamani Pedram, M.; Shahidzadeh, M.; Amini-Fazl, M. S. Evaluation of the catocene/graphene oxide nanocomposite catalytic activity on ammonium perchlorate thermal decomposition. *Int. J. Chem. Kinet.* **2019**, *51*, 337−345.
(31) Georgakilas, V.; Tiwari, J. N.; Kemp, K. C.; Perman, J. A.; Bourlinos, A. B.; Kim, K. S.; Zboril, R. Noncovalent Functionalization of Graphene and Graphene Oxide for Energy Materials, Biosensing, Catalytic, and Biomedical Applications. *Chem. Rev.* **2016**, *116*, 5464−5519.
(32) Yang, D.; Mo, W.; Zhang, S.; Li, B.; Hu, D.; Chen, S. A graphene oxide functionalized energetic coordination polymer possesses good thermostability, heat release and combustion catalytic performance for ammonium perchlorate. *Dalton Trans.* **2020**, *49*, 1582−1590.
(33) Zheng, C.; Qian, Q.; Liu, Y.; Ma, C.; Hong, J.; Li, S.; Chen, X. Synthesis, Crystal Structure and Characterizations of New 3,4,7,8-Tetrachloro-1,10-Phenanthroline Zn(II) Complex. *J. Chem. Crystallogr.* **2010**, *40*, 19−24.
(34) Guo, Z.; Liu, X.; Chen, X.; Zhang, C.; Yang, G.; Zhang, Y.; Ma, H. Design and synthesis of two energetic coordination polymers based on copper ion and 1H,1′H-[5,5′-bitetrazole]-1,1′-diol: A comparative study of the structure-property relationships. *J. Solid State Chem.* **2018**, *268*, 55−61.
(35) Wang, Y.; Yi, L.; Yang, X.; Ding, B.; Cheng, P.; Liao, D.; Yan, S. Synthesis, Crystal Structure, and Characterization of New Tetranuclear Ag(I) Complexes with Triazole Bridges. *Inorg. Chem.* **2006**, *45*, 5822−5829.
(36) Blaine, R. L.; Kissinger, H. E. Homer Kissinger and the Kissinger equation. *Thermochim. Acta* **2012**, *540*, 1−6.
(37) Kou, Y.; Song, X.; Guo, K.; Cheng, Z.; Wang, Y. Characterization, Thermolysis, and Energetic Properties of an MTNP/PETN Eutectic Prepared via the Solvent/Anti-Solvent Method. *Propellants, Explos., Pyrotech.* **2021**, *46*, 299−308.
(38) Song, X.; Guo, K.; Wang, Y.; Li, F. Characterization and Properties of F_{2602}/GAP/CL-20 Energetic Fibers with High Energy and Low Sensitivity Prepared by the Electrospinning Method. *ACS Omega* **2020**, *5*, 11106−11114.
(39) Zhang, K.; Fan, J.; Wang, X.; Xiaojun, F. Preparation, Structure and Performance of TKX-50/AP/GO Composite. *2021 International Conference on Development and Application of Carbon Nanomaterials in Energetic Materials*, 2022.
(40) Feng, C.; Ye, B.; An, C.; Zhang, F.; Hong, Z.; Wang, J. Preparation of functionalized GO coordination compound and its catalytic performance for thermal decomposition of ammonium perchlorate. *J. Mater. Sci.* **2021**, *56*, 19599−19613.
(41) Hao, G. Z.; Liu, J.; Gao, H.; Xiao, L.; Qiao, Y.; Jiang, W.; Zhao, F. Q.; Gao, H. X. Preparation of Nano-sized CuO and Its Catalytic effect on the thermal decomposition of AP. *Chin. J. Explos. Propellants* **2015**, *38*, 18.
(42) Dong, H.; Li, G.; Zhang, C.; Luo, Y. Preparation of CuO/PG Nanocomposites and Their Effect on the Catalytic Decomposition Performance of AP. *Chin. J. Energ. Mater.* **2018**, *26*, 1031−1037.
(43) Pei, J.; Zhao, H.; Yang, F.; Yan, D. Graphene Oxide/Fe_2O_3 Nanocomposite as an Efficient Catalyst for Thermal Decomposition of Ammonium Perchlorate via the VacuumFreeze-Drying Method. *Langmuir* **2021**, *37*, 6132−6138.

https://doi.org/10.1021/acsomega.3c01865
ACS Omega 2023, 8, 22876−22886